

Earth's Magnetic Field

- Description

- Geometry
 - Inclination and declination
- Strength
- Dipole and non-dipole
- Variability
- Geocentric Axial Dipole hypothesis

- Origin

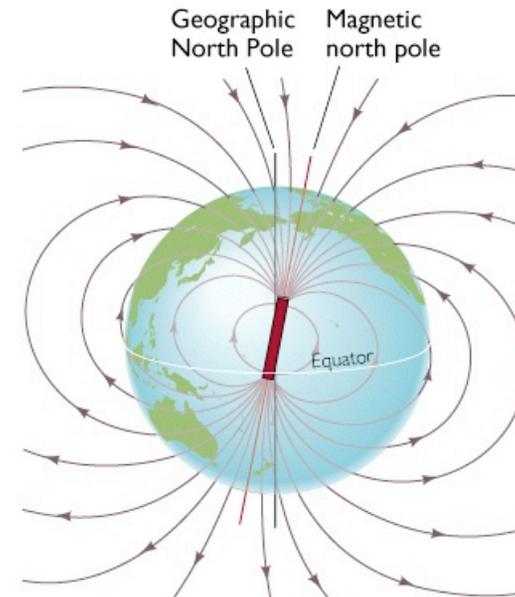
- Energy sources
- MHD
- Geodynamo
- Reversals

- Measurements

- Flux-gate
- Proton precession
- SQUID

- Rock Magnetism

- Physics of Magnetization
 - induced and remnant magnetization
 - Magnetization hysteresis
 - TRM, DRM, CRM, and IRMs
- Determination of GMP, VGP, paleo-pole, paleo-latitudes, and APW
- Geophysical exploration: measuring magnetic fields



Magnetic Field of the Earth

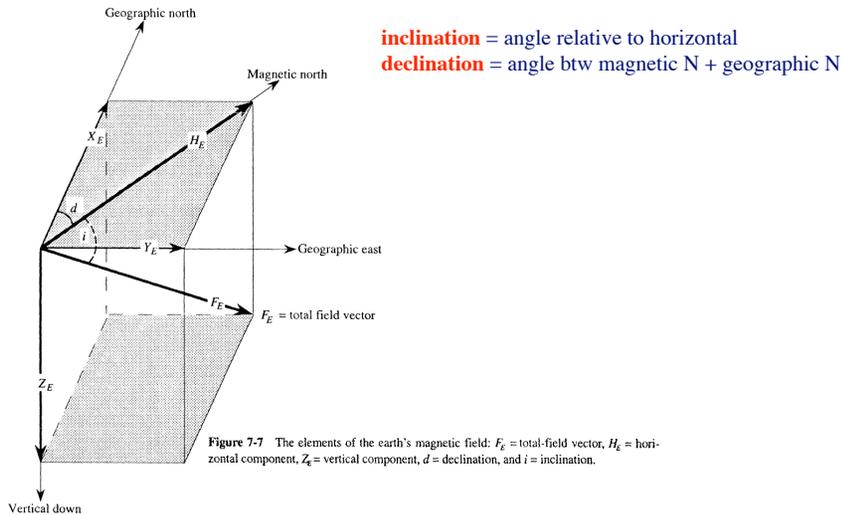
at magnetic dip poles
intensity is $\sim 70,000$ nT

at magnetic equator
intensity is $\sim 25,000$ nT
1 nT = 1 gamma (cgs)

Note direction relative to surface

Earth's magnetic field

At any location the magnetic field is a vector with magnitude (intensity) + direction

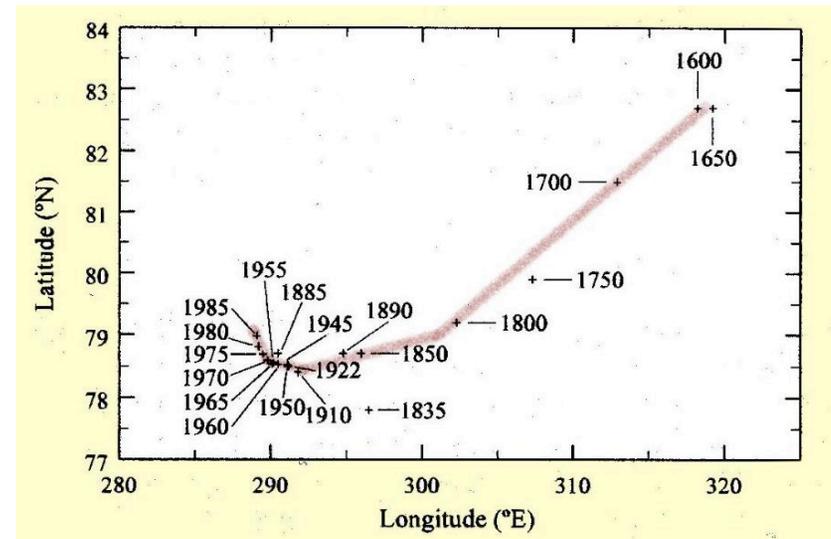


Earth Magnetic Variability

- External (solar and magnetosphere)
 - Magnetospheric substorms, daily solar variation, solar storms, sun spot cycle
 - 1 nT to 100 nT
- Internal (secular variation)
 - Intensity (-5% in last 100 years)
 - declination/inclination due to GMP movement
- Reversal Chronology

magnetics

- **B** and **H**: Same except for constant in free space ($\mathbf{B} = \mu_0 \mathbf{H}$), differ inside magnetic material ($\mathbf{B} = \mu_0 \mathbf{H}_{\text{ex}} + \mathbf{J}_{\text{int}}$). Both have been called “magnetic field”. We will call **H** the “Magnetizing Field”
- Total field vector **B** has vertical component **Z** and horizontal component **H**. (not to be confused with the magnetizing field)
 - Inclination, $I = \tan^{-1} Z/H$
 - $\tan I = 2 \tan(\text{latitude})$
 - Declination of **H** measured relative to true north
- Measured using
 - Flux-gate (component) or proton precession (total field) - .1 nT
 - SQUID (Superconducting Quantum Interference Device) all three components to very high precision (aT - 10^{-18} T) refrigerator magnet 10^{-2} T



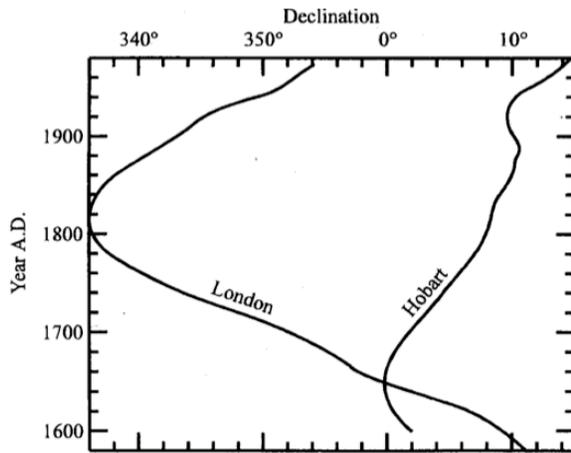
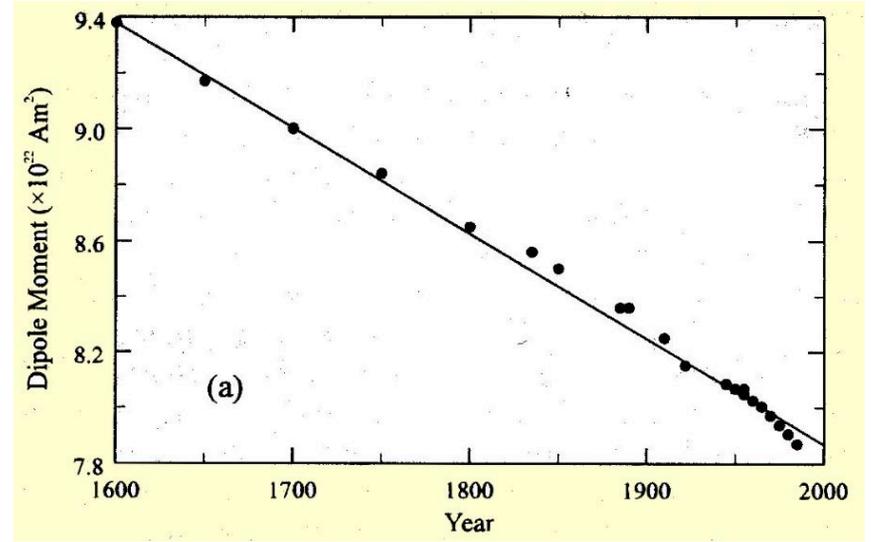
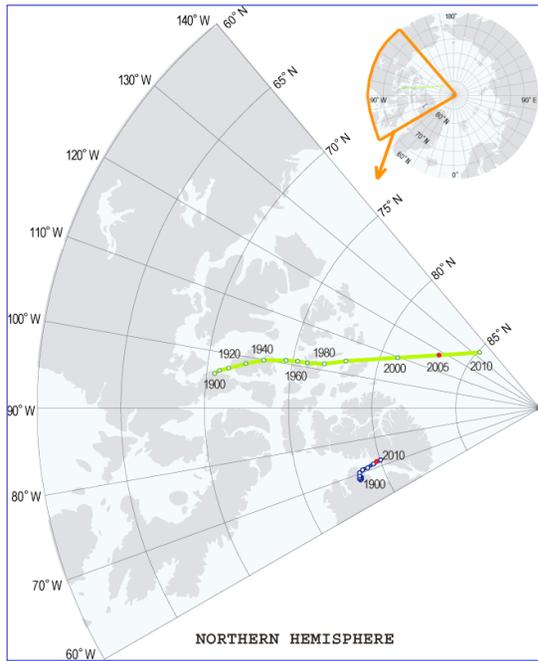


Fig. 2.8. Variation in declination at London, England (51.5°N), and at Hobart, Tasmania (42.9°S), from observatory measurements. The earliest measurement in the Tasmanian region was made by Abel Tasman at sea in 1642 in the vicinity of the present location of Hobart. Preobservatory data have been derived also by interpolation from isogonic charts.

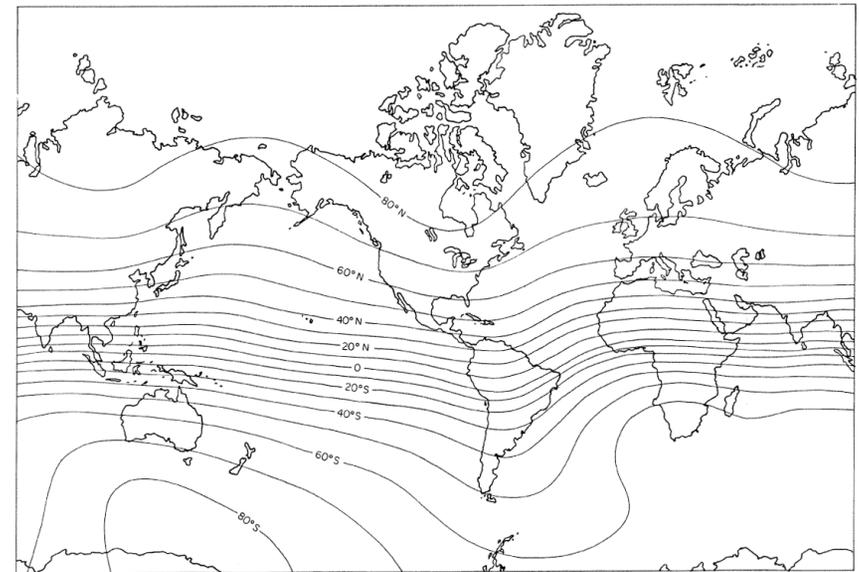


Figure 10-23 Main magnetic field inclination (solid contours) on the surface of the earth expressed in degree units. (Modified from "Magnetic Inclination or Dip," Epoch 1975.0, chart published by Defense Mapping Agency Hydrographic Center, Washington, D.C.) Robinson & Coruh

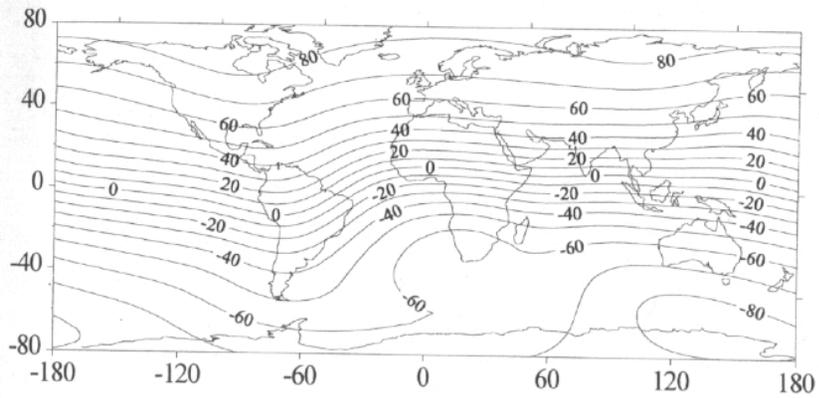


Fig. 2.3b. Isoclinic chart for 1990 showing the variation of inclination in degrees over the Earth's surface.

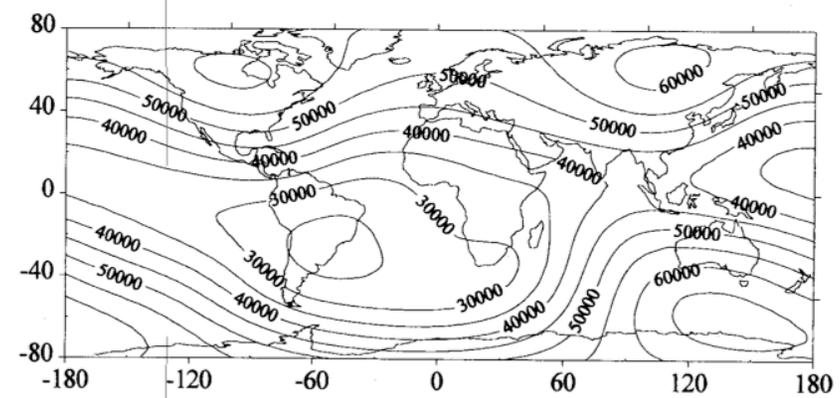


Fig. 2.3c. Isodynamic chart for 1990 showing the variation of total intensity over the Earth's surface. Contours are labeled in nT.

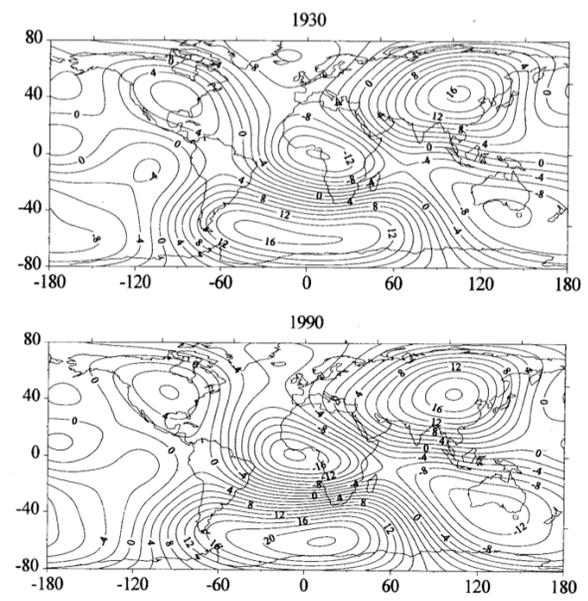
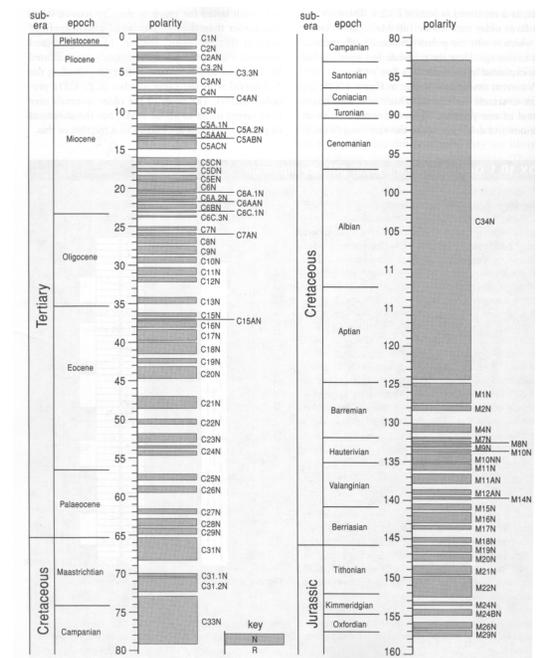


Fig. 2.10. The vertical component of the nondipole field for 1930 and 1990. Contours are labeled in units of 1000 nT.



Origin of Earth's Field

- Ideas that don't work:
 - Permanent Magnetization
 - Residual Currents
 - Thermoelectric effect
 - Gyromagnetic effect
 - Hall effect
 - Induced from external sources
 - More
- Only plausible remaining idea: Dynamo

Dynamo Theory: The Equations

- Maxwell's equations (E&M relationships)
- Ohm's Law (relationship between current & applied field)
- Navier-Stokes (fluid flow equations)
- Gravitational equation
- Heat Productions and transport
- Equation of state
- Continuity equation

$\nabla \times \mathbf{H} = \mathbf{J} + \frac{\partial \mathbf{D}}{\partial t}$	} Maxwell's equations	(8.1.9)			
$\nabla \times \mathbf{E} = -\frac{\partial \mathbf{B}}{\partial t}$		(8.1.10)			
$\nabla \cdot \mathbf{B} = 0$		(8.1.11)			
$\nabla \cdot \mathbf{D} = \rho_e$		(8.1.12)			
$\mathbf{J} = \sigma \mathbf{E} + \sigma(\mathbf{v} \times \mathbf{B})$	} Ohm's Law	(8.1.13)			
$\rho \left(\frac{\partial}{\partial t} + \mathbf{v} \cdot \nabla \right) \mathbf{v} + 2\rho(\boldsymbol{\Omega} \times \mathbf{v})$	} Navier-Stokes' equation	(8.1.14)			
$= -\nabla P + \eta \nabla^2 \mathbf{v} + \frac{1}{3} \eta \nabla(\nabla \cdot \mathbf{v}) - \rho \nabla \phi_g + \mathbf{J} \times \mathbf{B}$					
$\nabla \cdot (\rho \mathbf{v}) + \frac{\partial \rho}{\partial t} = 0$	} Continuity equation	(8.1.15)			
$\nabla^2 \phi_g = -4\pi G \rho$	} Poisson's equation	(8.1.16)			
$\frac{\partial T}{\partial t} = k_T \nabla^2 T + (\nabla k_T \cdot \nabla T) - \mathbf{v} \cdot \nabla T + \varepsilon$	} Generalized heat equation	(8.1.17)			
$\rho = \text{Function}(P, T, H)$	} Equation of state	(8.1.18)			
<table style="width: 100%; border: none;"> <tr> <td style="width: 30%;"><i>Notation:</i></td> <td style="width: 40%;"> H = magnetic field B = magnetic induction J = electric current E = electric field D = electric displacement vector v = velocity η = viscosity ρ_e = electric charge density $\boldsymbol{\Omega}$ = angular velocity of rotation </td> <td style="width: 30%;"> ρ = material density σ = conductivity T = temperature P = pressure G = gravitational constant ϕ_g = gravitational potential ε = heat source term k_T = thermal diffusivity </td> </tr> </table>			<i>Notation:</i>	H = magnetic field B = magnetic induction J = electric current E = electric field D = electric displacement vector v = velocity η = viscosity ρ_e = electric charge density $\boldsymbol{\Omega}$ = angular velocity of rotation	ρ = material density σ = conductivity T = temperature P = pressure G = gravitational constant ϕ_g = gravitational potential ε = heat source term k_T = thermal diffusivity
<i>Notation:</i>	H = magnetic field B = magnetic induction J = electric current E = electric field D = electric displacement vector v = velocity η = viscosity ρ_e = electric charge density $\boldsymbol{\Omega}$ = angular velocity of rotation	ρ = material density σ = conductivity T = temperature P = pressure G = gravitational constant ϕ_g = gravitational potential ε = heat source term k_T = thermal diffusivity			

Magnetic Induction Equation

- Maxwell's equation plus Ohms law
- Kinematic approach

Time dependence

$$\frac{\partial \mathbf{H}}{\partial t} = \frac{1}{\sigma \mu_0} \nabla^2 \mathbf{H} + \nabla \times (\vec{v} \times \vec{H})$$

Decay

Build up due to fluid motion

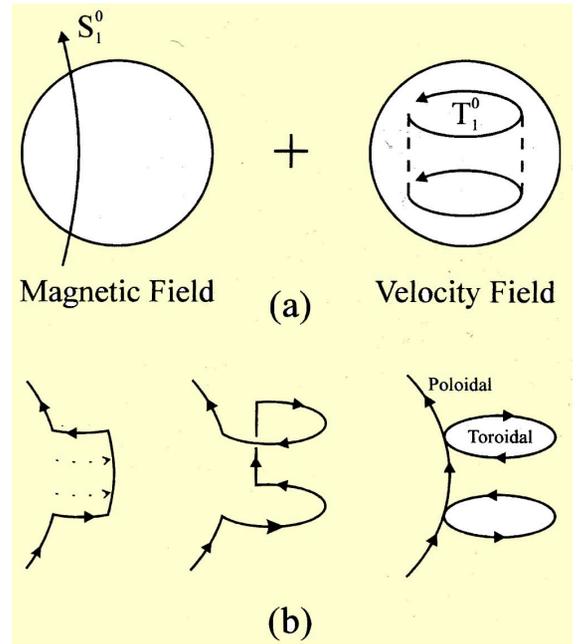
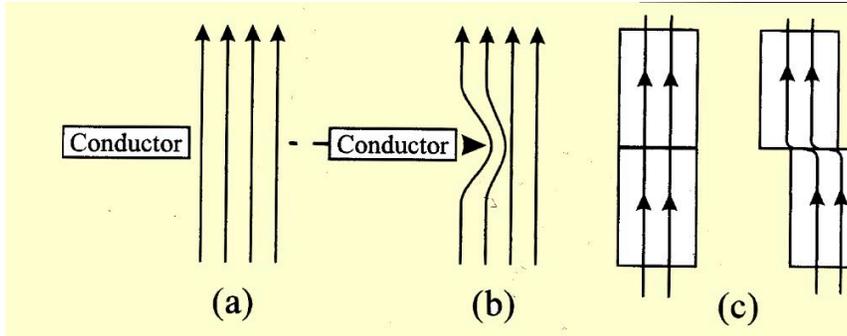


Fig. 8.8. Production of a poloidal magnetic field. A region of fluid upwelling, illustrated by dotted lines on the left, interacts with a toroidal magnetic field (solid line). Because of the Coriolis effect (northern hemisphere) the fluid exhibits helicity, rotating as it moves upward (thin lines, center). The magnetic field line is carried with the conducting liquid and is twisted to produce a poloidal loop as on the right. After Parker (1955a.)

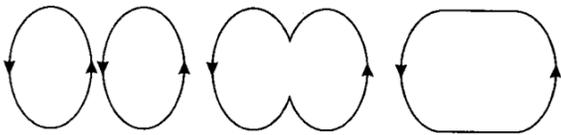
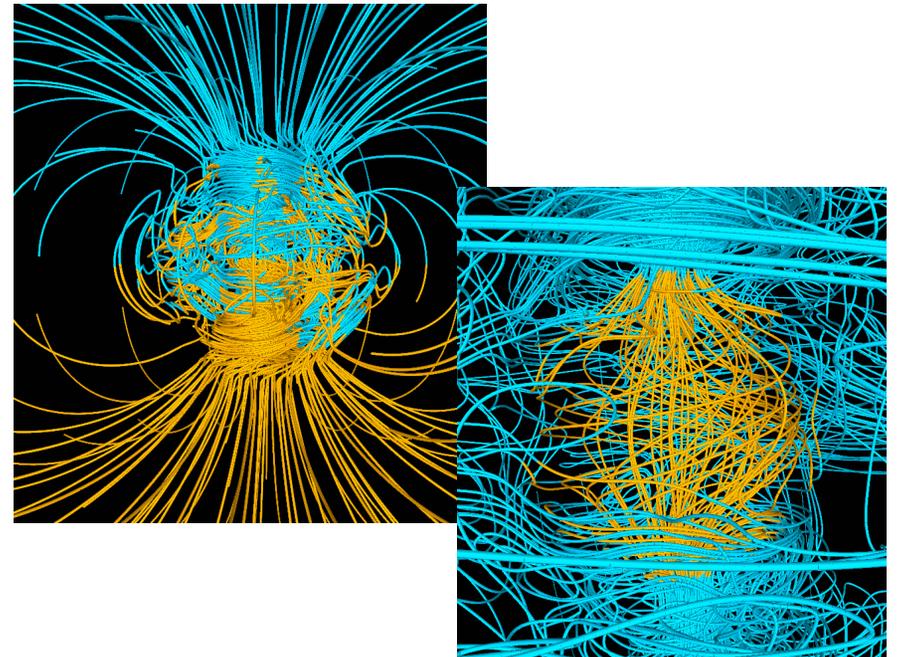
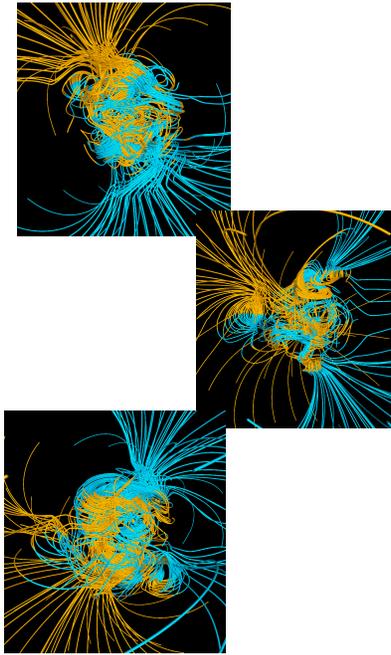


Fig. 8.9. Convergence of two poloidal loops as produced in Fig. 8.8 results in a larger poloidal loop. After Parker (1955a.)



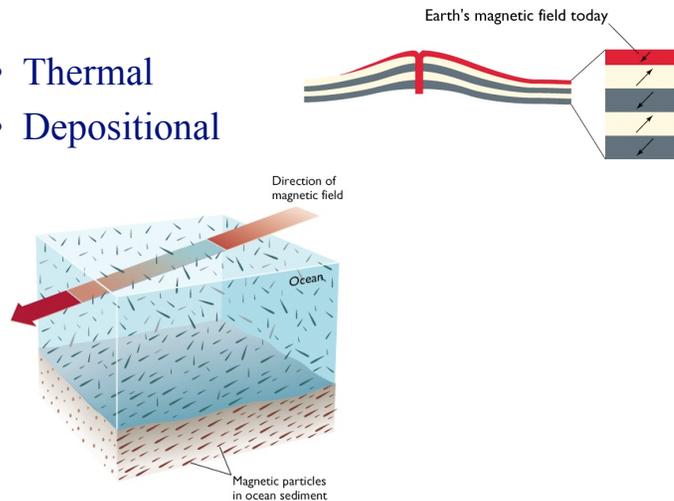


Rock Magnetism

- Requires “unpaired” electrons in material
- Paramagnetism and ferromagnetism
- Magnetic hysteresis
 - Induced magnetism
 - Remnant magnetism

Remnant Magnetism

- Thermal
- Depositional



Secondary Remanent magnetism

- Isothermal remanent magnetism IRM Strong field
eg. lightning strike
- Chemical remanent magnetism CRM (formation of new minerals)
- Viscous Remanent Magnetism VRM expose a rock to a field for a long time
- VRM adds noise to other magnetic signals in rocks, but can be removed by exposing the rock to an AC field of increasing strength.

Magnetization of Ocean Crust

Historical development

Remanent magnetization of igneous rocks was studied in early 1900's
Brunhes, Matuyama, others found weak but stable remanence
 concluded this was locked in when sample was last heated
 = **thermoremanent magnetization**
 occurs at unique **Curie temperature**

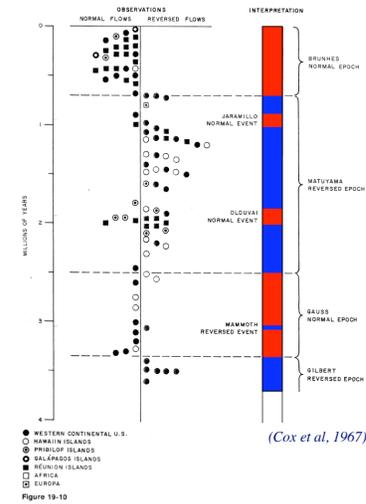
TABLE 12-2 Susceptibility and Curie Temperature of Some Important Ferrimagnetic Minerals

MINERAL	SUSCEPTIBILITY (emu)	CURIE TEMPERATURE (°C)
Magnetite	0.3-0.8	580
Ilmenite	0.135	50-300
Pyrrhotite	0.125	320
Maghemite	variable	545-675

Robinson & Coruh

most studies were restricted to late Pleistocene/archeological samples

Researchers looked at older samples for next 50 years
 frequently found reverse magnetization
 striking absence of 'in-between' orientations
 huge majority were either normal or reversed



~100 dates/polarities from terrestrial volc rocks around world identified
 4 major epochs + 3 shorter 'events'

(Cox et al., 1967)

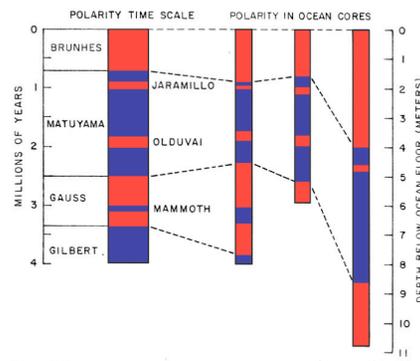
Though not understood, studies extended to magnetic reversals in marine sediments

Coring in 1950's focussed on deep sea sediments for many reasons
 Same terrestrial reversal time scale detected in deep sea sediments

≠ **thermoremanence**

= physical alignment of detrial grains having remanent magnetism
 called '**detrital remnant magnetization**'

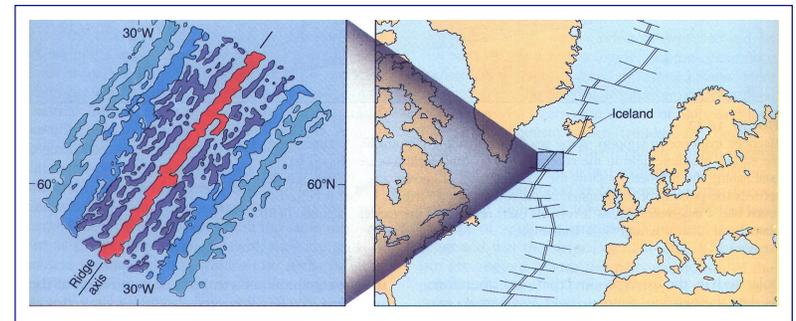
Measured with '**spinner magnetometer**'
 oriented sample placed on rotating spindle
 external field is masked
 permanent mag of spinning sample
 creates current in surrounding coil
 strength of current + coil/sample
 orientation reveal original field



(Cox et al., 1967)

Figure 19-11 Deep-sea sediments confirm the field-reversal time scale. Magnetic particles become oriented in the direction of the earth's field as they settle through the water; a core that samples many layers of sediments may record a series of normal (gray) and reversed (light) epochs and events. Here cores from antarctic waters are correlated with the time scale

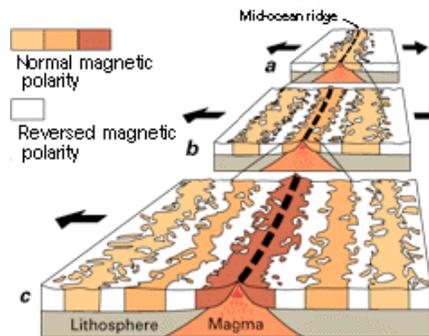
Soon after, symmetric mag anomalies were detected on either side of Mid-Atl Ridge
 obviously non-random controlling process
Hess ('62) put it together in suggesting crust forms by solidifying at MOR



Symmetric magnetic lineations across the Mid-Atlantic Ridge caused by alternating total field

Magnetization of ocean floor basalts

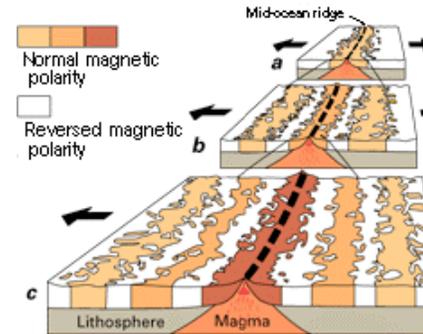
- ocean floor basalts retain a high TRM
- large quantity of magnetite grains and small grain size promote high TRM
- ocean floor basalts are produced by continuous mid-ocean ridge volcanism



- basalt crystallizes fast, forms Layer 2, with a high TRM
- strips of Layer 2 with alternating normal and reversed polarity form
- progressively age away from the spreading centre.

Magnetization of ocean floor basalts

- in strips that formed during normal polarity, the remnant magnetization adds to the induced field
- this produces a positive magnetic anomaly
- in strips that formed during reversed polarity, the remnant magnetization subtracts from the induced field
- this produces a negative magnetic anomaly



- when the anomalies are contoured, the effect is to produce stripes of alternating high (positive) and low (negative) magnetic intensity
- the ocean floor "magnetic stripes".

Ocean crust as a tape recorder of thermoremanent magnetization
 vertical reversal time scale is laid out horizontally

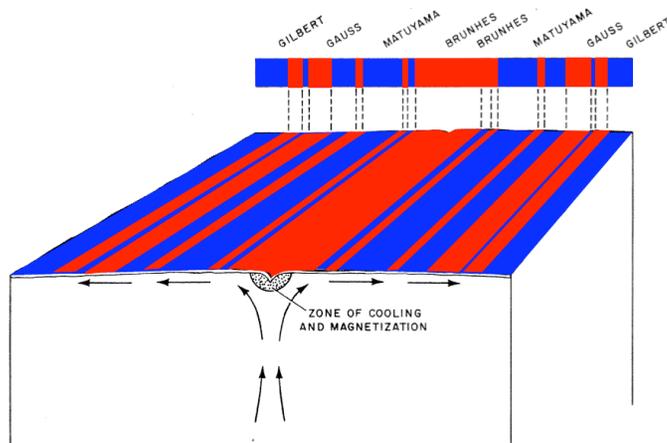


Figure 19-14

(Cox et al, 1967)

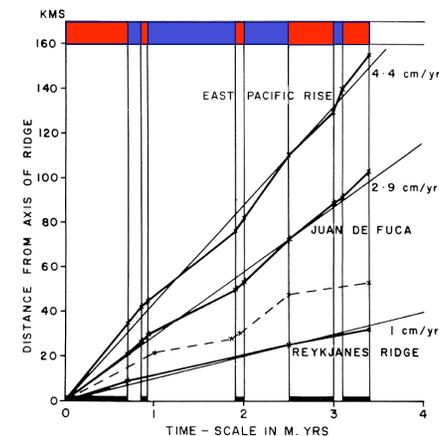


Figure 24-11
 Inferred normal-reverse boundaries within the crust plotted against the reversal time scale of Figure 24-4. The dashed line represents a similar plot for Juan de Fuca Ridge, if one assumes the earlier time scale—as did Vine and Wilson (1965). Note the similar deviations from linearity for the East Pacific Rise and Juan de Fuca Ridge (Vine, 1966)

Magnetization of ocean floor basalts

Soon the reversal time scale was extended to 11 Ma
e.g., the East Pacific Rise out to 500 km, 11 Ma

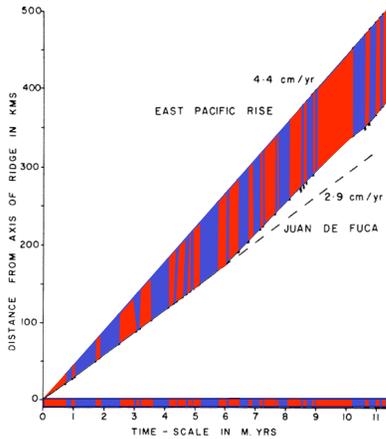
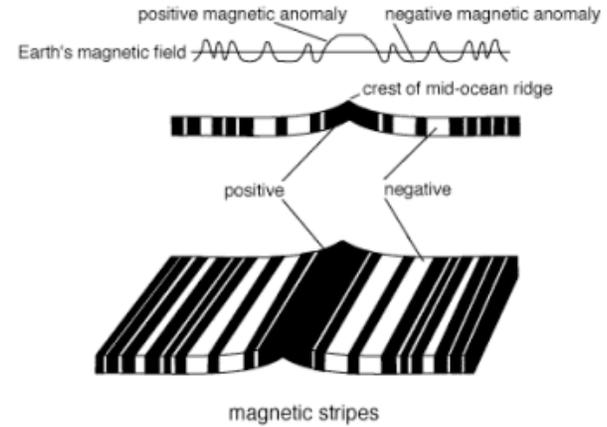


Figure 24-13
 Magnetic boundaries across the East Pacific Rise, deduced out to 500 kilometers from the crest and plotted on a line representing a constant spreading rate of 4.4 centimeters per annum. Similar boundaries from Juan de Fuca Ridge are plotted out to 150 kilometers on the assumption of a constant spreading rate of 2.9 centimeters per annum. The time scale out to 5.5 million years is based on both plots. Beyond that time the time scale is based on the East Pacific Rise boundaries, and those deduced from Juan de Fuca Ridge are simply plotted on these time lines (Vine, 1966)

- shape of magnetic anomalies best expressed on a line graph:



Observed + modeled anomalies
 EPR, Juan de Fuca + model – *good match*
 100km = 4Ma
 25km/Ma
 $25 \times 10^5 \text{ cm} / 10^6 \text{ yr}$
 2.5cm/yr
 note the 8 km source layer
 500 Gammas = 500 nT

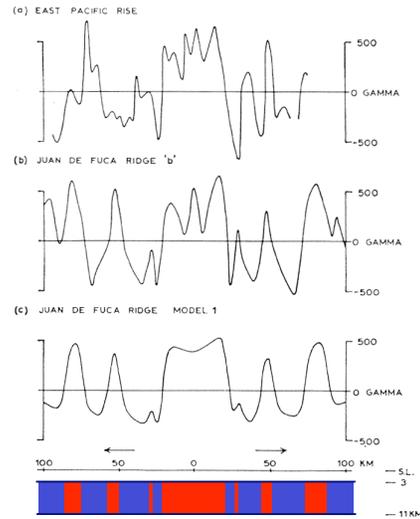
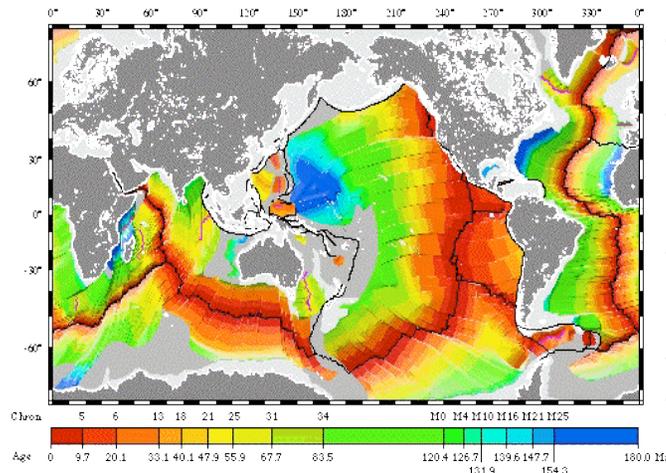


Figure 23-2
 (a) Observed profile across the East Pacific Rise at 59°S, 149°W (Heizler, 1961). (b) Observed profile 'b' across the Juan de Fuca Ridge (see Figure 23-4). (c) Model and calculated anomaly for Juan de Fuca Ridge, assuming generalized crustal blocks (compare Figure 23-1c) (Vine and Wilson, 1965)

Ocean Floor map



- oldest ocean floor
- fast versus slow sea-floor spreading
- subducted mid-ocean ridges
- Iceland
- back arc areas = young
- former ocean ridges (Labrador Sea, NE Indian Ocean).